Pharmaceutical Research, Vol. 22, No. 7, July 2005 (© 2005)
DOI: 10.1007/s11095-005-5647-z

Research Paper

Characterization of Drug Particle Surface Energetics and Young's Modulus by Atomic Force Microscopy and Inverse Gas Chromatography

Michael Davies,[1] Anne Brindley,[2] Xinyong Chen,[1] Maria Marlow,[2] Stephen W. Doughty,[1] Ian Shrubb,[2] and Clive J. Roberts[1,3]

Received February 15, 2005; accepted April 25, 2005

Purpose. Particulate interactions are dominated by aspects such as surface topography, exposed chemical moieties, environmental conditions, and thermodynamic properties such as surface free energy (γ). The absolute value and relative magnitude of surface energies of a drug and excipients within a formulation can significantly influence manufacture, processing, and use. This study utilizes and compares the potentially complementary analytical techniques of atomic force microscopy (AFM) and inverse gas chromatography (IGC) in the quantitative determination of the surface energy of drug (budesonide) particles (micronized and unmilled) relevant to inhaled delivery. In addition, the study investigates with AFM another important parameter in determining material interactions, the local mechanical properties of the drug.

Methods. AFM was used to acquire force of adhesion (F_{adh}) and related work of adhesion (W_A) and surface energy values between individual mironized drug particles and also model substrates (graphite and mica). In addition, AFM probes were used to interrogate the surface energy of unmilled drug particles. Measurement with AFM probes also yielded localized measurements of Young's modulus for the unmilled drug. IGC was also used to probe the surface characteristics of the bulk drug material.

Results. The average values for surface energies acquired from budesonide micronized particle interactions with graphite, mica, and drug particles of the same substance were found to range from 35 to 175, 5 to 40, and 10 to 32 mJ m^{-2}, respectively. The unmilled material displayed a range of values of 39–88 mJ m^{-2} with an average of 60 mJ m^{-2}. The IGC result for the surface energy of the micronized material was 68.47 ± 1.60 mJ m^{-2}. The variability in surface energy from AFM, a feature particularly apparent for the micronized material was attributed to two factors, intrinsic material variations within a single particle and assumptions present within the contact mechanics model used. Here we provide a detailed description of these factors to go some way to rationalize the results. The Young's modulus of the unmilled drug was determined to be approximately 10 GPa.

Conlusion. The range of determined surface energies between the AFM measurement on graphite, mica, and the drug is proposed to reflect the different chemistries displayed by the drug at the single particle level. The maximum values of these ranges can be related to the sites most likely to be involved in adhesion. AFM and IGC yield surface energy estimates in approximate agreement, but clearly are interrogating surfaces in different fashions. This raises questions as to the nature of the measurement being made by these approaches and to the most appropriate time to use these methods in terms of a direct relation to formulation design, manufacture, and drug delivery. Finally, we demonstrate a novel method for assessing the Young's modulus of a drug from a single particle.

KEY WORDS: AFM; force of adhesion; hardness; IGC; surface free energy; work of adhesion; Young's modulus.

INTRODUCTION

Inhaled drug delivery has been used for many years as a mode to deliver therapeutic agents to the lung to treat respiratory disorders (1), such as asthma. To achieve pulmonary delivery, the pharmacologically active agent must first be aerosolized. An aerosol may be described as a dispersion of solid or liquid particles within a gaseous system (2). Traditionally pressurized metered dose inhalers (pMDIs) have been the devices of choice to deliver aerosolized preparations containing a drug substance to the lungs. In recent years, the desire to avoid the need for propellants has resulted in the development of dry powder inhalers (DPIs) (3).

To ensure effective drug targeting to the lung from inhaler systems, it is of importance to have an understanding of their formulation parameters, such as drug particle physicochemical properties, and interactions. Particle adhe-

[1] Laboratory of Biophysics and Surface Analysis, School of Pharmacy, The University of Nottingham, NG7 2RD Nottingham, UK.
[2] AstraZeneca R&D Charnwood, Pharmaceutical & Analytical R&D, LE11 5RH Loughborough, UK.
[3] To whom correspondence should be addressed. (e-mail: clive.roberts@nottingham.ac.uk)

sion and interactions occur at all stages of the inhalation process, typically within the delivery device, throughout movement into the respiratory tract, and also during particle deposition and interaction with pulmonary fluid. The extent of particle interaction is governed by a number of forces that occur between the material and the substrate it contacts (4), the principal forces being van der Waals, electrostatic, and capillary forces (5). It is well known that such forces are significantly influenced by numerous parameters, including particle morphology, surface chemistry, and free energy (6). In addition, the control and effect of environmental factors including humidity and temperature are often critical (7).

Interparticulate forces have been successfully investigated via centrifugation techniques (8); however, certain drawbacks to this approach exist such as the small particles associated with pulmonary delivery are often difficult to investigate and certain factors influencing the interaction cannot be studied (6). It is also difficult to quantify fundamental forces occurring between individual particles. The application of the atomic force microscope (AFM) in recent years to the study of single particle interactions has offered a method capable of addressing many of these issues (9–11). AFM directly interrogates adhesion in an environment that can be tailored to the application [e.g., humidity (12–14) and solvent (15–17)]. So, for example, AFM can be used to provide an excellent insight into properties and delivery of inhaled drug particles. The approach can be tailored to investigate systems such as particle–particle interactions within DPIs, particle–DPI wall interactions, and to also perform *in vivo* simulations of relevance to the pharmaceutical industry, for instance, inhaled particle–pulmonary surfactant interactions. For example, Sindel *et al.* have applied AFM both qualitatively and quantitatively to study forces of interaction between lactose substrates (18). This investigation established the morphology of contacting asperities and directly related this characteristic to the force of adhesion (F_{adh}). Of particular relevance here is the recent development of a suitable AFM-based method for the quantitative determination of the work of adhesion (W_A) between salbutamol particles and a flat substrate by AFM (19). This methodology is based on assessing the true contact area between rough particles to allow the determination of the surface energy (γ) of formulation components from individual particles. The determination of γ is a recognized step in predicting a range of properties that may be displayed by a powder, including, for example, adhesion (20) and binder performance (21).

As a method for determining γ directly from the force required to separate particulates [note the similarity to the definition of W_A, as the energy required to separate 1 m^2 of an adhering surface in a vacuum (22)], AFM seems quite different from alternative approaches that determine the same parameter, such as Wilhelmy plate-based techniques (23), liquid penetration of a powder bed (24), isothermal microcalorimetry (25,26), and inverse gas chromatography (IGC) (27,28).

The W_A between two materials (a and b) and γ can be related via Eq. (1). The γ can be expressed as the free energy change during an increase in surface area by 1 unit (29). In general, the larger the γ term, the greater the adhesion force experienced (30). An interfacial γ (γ^{ab}) will exist at the point of contact between two materials, the extent of which will be governed by the individual γ of the contacting materials (29,31). The interfacial γ value will have a significant impact upon features such as adhesion (31).

$$W_A = \gamma^a + \gamma^b - \gamma^{ab} \quad (1)$$

IGC is a highly sensitive, quantitative analytical technique employed to explore and determine the nature of powder surfaces, in particular those relevant to the pharmaceutical industry (30,32). This approach may be used to probe surfaces and elucidate important thermodynamic properties of the sample under study, such as the γ (33). When considering IGC data, the γ term is divided into two components: polar and dispersive elements Eq. (2)—where the dispersive term (γ^d) relates to nonpolar and the polar parameter (γ^p) refers to hydrogen bonding and acid–base forces (31). The dispersive component of the γ is generally considered of greater significance than the polar element (29).

$$\gamma = \gamma^p + \gamma^d \quad (2)$$

IGC is well suited to the role of assessing bulk material surface characteristics as it is nondestructive and considers only the outermost layer of the sample (33), i.e., the region of the substance directly involved during interactions. This relatively new technique is now becoming a more established mode to explore powder surface characteristics (34). This approach may be readily applied in the investigation of surface properties or for in-process evaluation of a sample of drug particles obtained during manufacture and those typically found in DPI reservoirs. The ability to immobilize the material within a chromatography column in a similar fashion as it would exist during production, manufacture, and use is a powerful property of IGC. Ticehurst *et al.* highlighted the application of IGC in the study of batch variation of surface properties of α-lactose monohydrate (32). The work demonstrated that the batches under investigation were in fact different in terms of surface energetics, a feature not detected by conventional characterization methods such as X-ray diffraction and differential scanning calorimetry. It should be noted that to date the models used to derive surface energy from AFM-based adhesion measurements have only taken into account the apolar component of the surface energy.

The AFM approach used here to investigate surface energy lends itself with little modification for the concurrent determination of mechanical properties of particles. Taken together with surface energy measurements, knowledge of such properties provides additional insight into how particulates may interact and respond to processing that cause deformation during manufacture or delivery. Here we determine the Young's modulus of unmilled budesonide crystalline material. The use of the larger particles as compared to the micronized material facilitates the ability of the AFM probe to interact with a single particle on a flat planar region as is preferred for this type of measurement. Previously for pharmaceutical particulates, as considered here, such determinations have generally relied on traditional three-point bending of beams made of 20–200 mg of compacted material (35). It should be noted that AFM has previously been successfully employed to locally investigate the Young's modulus of cells (36,37), liposomes (38), polymers (39), and inorganic crystals (40).

In summary, the key aim of this study is to present quantitative AFM and IGC data relating to the surface energetics of inhaled drug particles of the same material, budesonide. AFM is also used to assess the spatial variation of surface energy across large, unmilled crystalline particles of the drug. From these data, an assessment of the complementarity, or not, of the approaches is made. Consideration is also afforded to the particular value of each technique in a pharmaceutical context. In addition, the study investigates with AFM another important parameter in determining material interactions, the local mechanical properties of the drug.

MATERIALS AND METHODS

Drug Substance

The work conducted during this study is based on micronized budesonide particles (BN 4652 M; AstraZeneca, Loughborough, UK) suitable for inhalation and unmilled budesonide (BN 300087-01, AstraZeneca). The compound may be described chemically as 11β, 21-dihydroxy-16α, 17α-propylmethylenedioxy-1,4-pregnadiene-3,20-dione (Fig. 1) (32). For the micronized material, at least 98% of the particles exhibit a diameter less than 7 μm, and 18–31% have a diameter of less than 1.5 μm (33). The presented scanning electron microscopy (SEM) image of uncoated material indicates typical particle sizes expected (Philips XL30 FEG ESEM; Philips, Eindhoven, The Netherlands). It is evident that the micronized sample is composed of crystalline, nonspherical particles, in addition to agglomerates (Fig. 2A). Figure 2B shows a typical SEM image of the unmilled budesonide; the large crystalline particles can be seen to be decorated with small particulates. The predominant face of the large crystalline particles is the (002) plane.

Micronized Drug Particle Attachment on AFM Cantilevers

Silicon nitride V-shaped cantilevers (Veeco, Santa Barbara, CA, USA) were utilized for the adhesion measurements conducted during this study. Prior to their use the spring constant of each cantilever was established via the thermal method (34) using a Molecular Force Probe AFM (Asylum Research, Santa Barbara, CA, USA). Micronized drug particles were attached to the apex of each cantilever using a Nanoscope IIIa MultiMode AFM (Veeco) via a previously reported procedure (35).

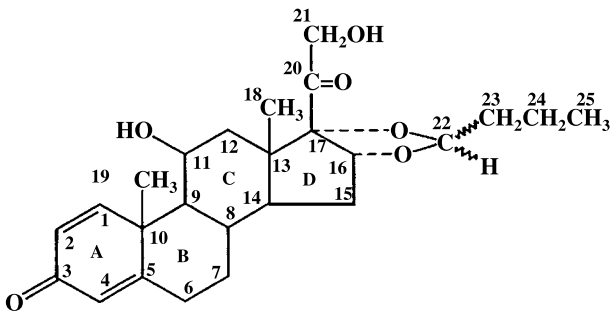

Fig. 1. The chemical structure of budesonide.

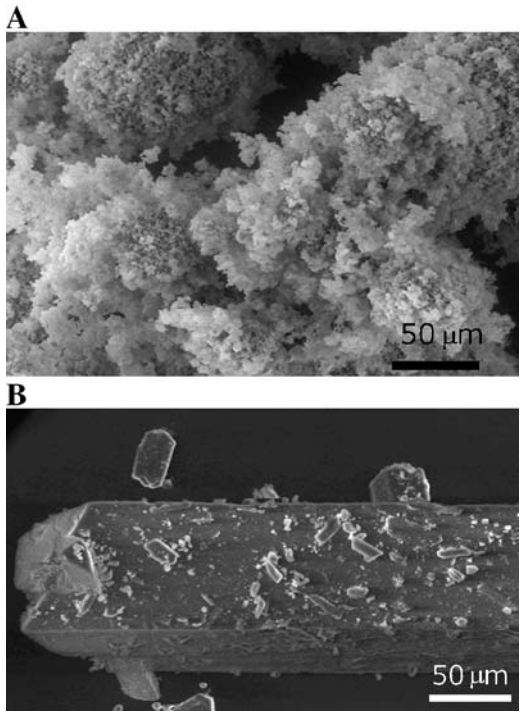

Fig. 2. (A) SEM image of micronized budesonide particles suitable for inhalation. (B) SEM image of the unmilled budesonide.

To ensure that drug particles had been successfully mounted onto the cantilever apex, the tips were subject to SEM analysis. The tips were placed on carbon disks attached to aluminum stubs designed for SEM use. The samples were not gold coated before imaging, as this would have rendered them useless for future force adhesion measurements. SEM analysis was carried out at an accelerating voltage of 2.5 kV and a spot size of 50 nm.

Further to completion of the adhesion analysis and particle morphology determination involving each system, the samples were again subject to SEM to ensure that these procedures had not unduly affected particle morphology or removed the particles completely from the apex of the AFM cantilever.

Force of Adhesion and Young's Modulus Measurements

An Explorer AFM (Veeco) was used to conduct adhesion and Young's modulus measurements. In addition, this instrument was also employed to generate topographical images relating to the morphology of the drug particles used. The substrates on which the adhesion measurements were conducted using cantilevers with micronized drug particles attached were freshly cleaved highly oriented pyrolytic graphite (HOPG) (Agar Scientific, Essex, UK), freshly cleaved Muscovite mica (Agar Scientific), and individual particles of the same drug substance (AstraZeneca) immobilized on double-sided tape. HOPG and mica were chosen as model substrates due to their high purity, chemically inertness, and flat surfaces at the nanoscale. These features enable the generation of reproducible adhesion data regardless of where the sample was positioned on the substrate. In ad-

dition, similar AFM cantilevers with no particle attached were employed to obtain force measurements across the predominant face of unmilled drug crystals, thus enabling both an estimation of the surface free energy for this material and an assessment of potential local variation in this parameter across the drug surface. A total of 100 adhesion measurements were acquired for each sample via application of force volume scans over an area of 10 × 10 μm on each substrate. The force volume scan is used to provide an insight into and map interaction forces occurring over specific regions of the substrate. All measurements were conducted at a temperature of 25°C and 0% relative humidity (RH).

For Young's modulus measurements on the unmilled drug, stiffer tapping mode tips (Olympus, Japan) of nominal spring constant 40 N/m were used. To provide the necessary calibration of cantilever response, the AFM probe was pressed onto silicon before force data were recorded from drug particles. The response obtained when the drug crystal is challenged by the AFM probe may be subtracted from the silicon value to generate the true force displacement parameter. During each set of measurements, the same AFM probe was used to directly compare data between the silicon and the drug; the optical laser alignment remained constant throughout. For each area of budesonide studied, a total of 100 force measurements were acquired from a 10 × 10 μm area.

Particle Contact Area Determination

The AFM probes functionalized with drug particles were imaged using a tip characterization grid (TGT01; NT-MDT, Moscow, Russia), which is composed of a series of repeating sharp spikes, using a method described by Hooton *et al.* (43). As the sample is passed over the spikes (scan rate of 10 μm/s), a topographical image of the particle surface is generated due to the spikes being in general sharper than the asperities present on the surface of interest—a process termed "tip imaging" (44). Multiple images of the particle are created that allows checks to be made on particle changes during this process. Further to the generation of the raw tip image data, each representation of the surface topology was processed using the Explorer AFM software (Version 4.01.b3, August 1, 1997, Topometrix Inc., Santa Clara, CA, USA). The images were initially passed through a median filter to reduce noise spikes and dropouts that could potentially affect image accuracy (45).

Cross-section profiles of the particle images and three-dimensional reconstructions were obtained using SPIP AFM image processing software (Image Metrology ApS, Lyngby, Denmark). To determine the contact surface area involved in adhesion events, force curves were inspected to estimate the range of interaction of each drug particle into each substrate. This range was taken as a function of the ordinate distance between the set point and the free level on the force curve.

Determination of W_A and γ

The contact surface area values obtained were used to calculate the work of adhesion, W_A, based on the assumption of a hemispherical contact geometry of radius R for the particle Eq. (3) (46).

$$W_A = \frac{3F_{adh}}{2\pi R} \tag{3}$$

where F_{adh} is the measured force of adhesion. Further to this step, Eq. (4) was applied to generate data relating to the γ of the drug particles (γ_1) utilizing the known γ of the model substrates (γ_2; for HOPG the value used was 100 mJ m^{-2} and for mica 4,500 mJ m^{-2}) (47). Where a blank AFM tip is pressed into the unmilled budesonide particles, the R term relates to the terminal radius of the AFM probe which is determined in the same fashion as for the particle on an AFM probe.

$$\gamma_1 = \frac{W_A^2}{4\gamma_2} \tag{4}$$

In the case where cohesion measurements were carried out, i.e., drug on drug, then $\gamma_1 = \gamma_2$ (29).

Determination of Young's Modulus

To estimate the Young's Modulus (E) of the crystalline material, the amplified Hertz model was employed (48). This model is based on the principle of an elastic sphere of radius, R, deforming a planar surface by δ. Equation (5) details the model.

$$E = \frac{3(1-\nu^2)k\Delta z}{4\delta^{3/2}R^{1/2}} \tag{5}$$

where ν is Poisson's ratio (taken to be 0.5), k is the spring constant of the AFM cantilever, and Δz is the relative piezoelectric scanner displacement. To obtain a value for δ and hence E, the difference between the gradient of the force data on the drug and the gradient on the hard silicon surface was determined following the method of Rotsch and Radmacher (36). The value of R was obtained in a similar manner as that described for particle contact radius using a tip characterization grating.

Inverse Gas Chromatography

A sample of the micronized budesonide particles was gently packed and immobilized in a presilanated IGC column of length 30 cm and internal diameter 3 mm. The column was then plugged with silanized wool and placed within the IGC apparatus (Surface Measurement Systems, Alperton, UK). Methane was employed as the reference probe and introduced into the system to remove the "dead volume." The IGC column was equilibrated for approximately 3 h prior to use. A total of four samples were taken from the same batch of inhaled drug particles and subsequently exposed to a series of precharacterized molecular probes (20 ml vapor: ethanol, acetone, ethyl acetate, chloroform, and 1,4-dioxane; Sigma, Gillingham, UK) within the infinite dilution range. The IGC apparatus was operated at a temperature of 30°C and 0% RH. The molecular probes were transported through the chromatography column at a rate of 10 ml min^{-1} and their retention times recorded. Helium was used as the carrier gas.

The retention times were then used to calculate the dispersive (γ_s^d) and specific ($-\Delta G^{SP}$) components of the γ by using the theoretical approach employed by Schultz and Lavielle (49).

RESULTS AND DISCUSSION

AFM Analysis

Budesonide Surface Energy Determination

SEM images for each AFM probe with budesonide particles were acquired both before and after all AFM adhesion measurements. Data were only used when it was clear that drug particles had been successfully attached to the apex of the cantilever and that no significant particle deformation or detachment had occurred after adhesion measurements and tip imaging protocols.

The forces of interaction between the drug particles and model substrates were investigated using force volume scans. This technique facilitates the generation of a predetermined number of force data relating to a specific region of the substrate; this information may be directly related to surface topology, if desired. A typical adhesion data set obtained using the model substrates mica is illustrated in Fig. 3 (HOPG data seems similar in form). With respect to the drug–drug system, it was evident that the force curves sometimes differed significantly from those obtained using the model substrates (Fig. 4). On occasion, these data displayed multiple adhesion points, as indicated by a number of troughs in the pull-off trace. This feature is to be expected, as the contacting drug particles would exhibit numerous undulations resulting in many contact points and thereby interactions at several different locations. In such cases the total W_A was determined as a sum of each of these interaction events.

The tip imaging protocol as described in the Material and Methods section was utilized to both gain an insight into the gross morphology of the contacting region(s) of each sample, thereby providing scope to generate contact surface area data, and also to confirm that adhesion data acquisition had not adversely affected the samples under investigation.

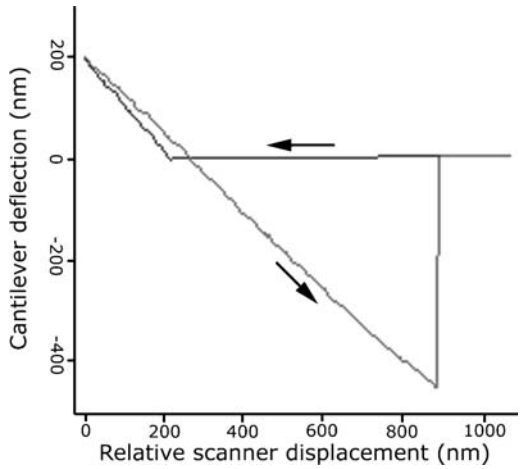

Fig. 3. An example force of adhesion data set acquired for a budesonide particle on an AFM probe challenged to a model mica surface.

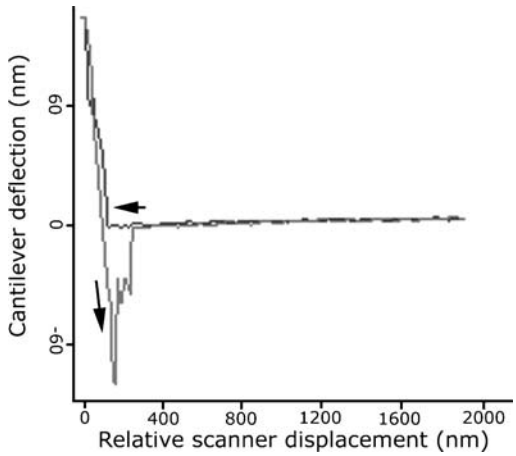

Fig. 4. A typical force of adhesion measurement obtained from a drug–drug particle interaction. Due to multiple interaction points and absence of a convening point of the approach and retract trace the W_A as determined by summing the individual events within the separation phase.

Tip images of an AFM cantilever with no drug particle attached (control) and representative drug particle samples and are presented in Fig. 5. It is evident that the structure of the control AFM tip (Fig. 5A) is dissimilar to the image with drug particle attached (Fig. 5B), indicating that the drug particle asperities would contact each substrate rather than the AFM tip itself.

The tip images obtained from the aforementioned process indicate that particle structural features are maintained throughout the study, overall ensuring the validity of the data acquired, i.e., one could not be sure of the reliability of the data if the overall morphology were to change significantly.

The W_A determined from the AFM adhesion data (from five different particles on AFM probes) on the drug–HOPG, the drug–mica, and the drug–drug systems ranged from 350 to 790, 220 to 520, and 20 to 90 mJ m^{-2}, respectively. The γ determined from the AFM adhesion data on the drug–HOPG, the drug–mica, and the drug–drug systems ranged from 35 to 175, 5 to 40, and 10 to 32 mJ m^{-2}, respectively. The observed ranges of W_A values for each pair of materials indicate that the relative interactions between each pair ranks as follows: drug–HOPG > drug–mica > drug–drug. We have quoted ranges of values as opposed to averages because the data reflect the localized work of adhesion or drug surface energy determined at the particle–sample contact point, which of course varies across an individual particle.

It should also be noted that the Johnson–Kendall–Roberts (JKR) (50) model used to determine the W_A makes a number of assumptions concerning the nature of the interacting material, and consequently has various well-known limitations; for example, the morphology and the localized roughness of the contact region are more complex than can be allowed for in our analysis. The fundamental principle on which this model is based is a scenario where a smooth sphere, with elastic properties, contacts a flat substrate (23). In the case of the work presented here, the systems under investigation do not reflect this situation (i.e., rough particles contacting substrates with different surface characteristics). Furthermore, the JKR theory only considers short-range

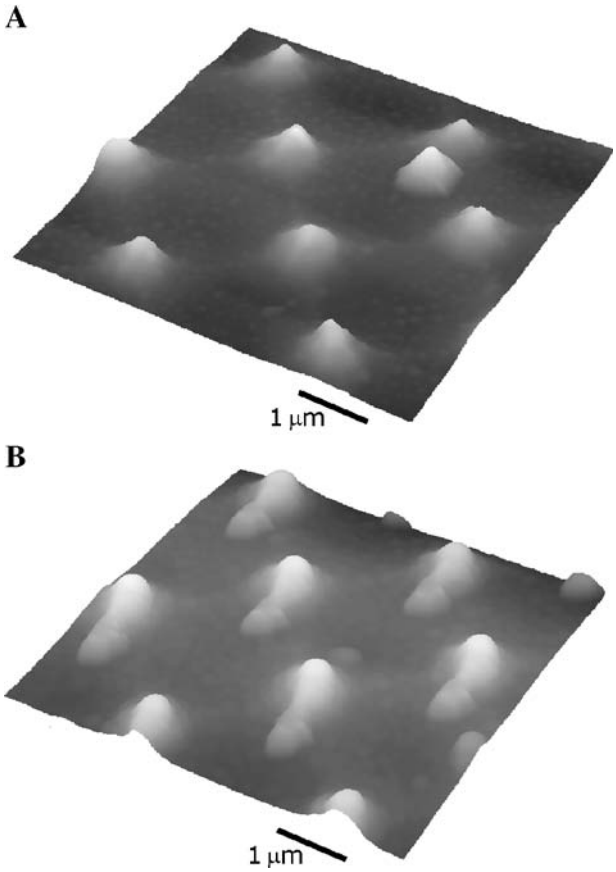

Fig. 5. Tip images of (A) control tip (XY = 5.7 μm, Z = 425 nm) and (B) drug particle asperity postmica adhesion measurements (XY = 5.7 μm, Z = 431 nm).

forces that act within the contact region, and therefore it neglects potential long-range forces that could exist outside the contact zone (29). As a consequence of this feature, the model accounts for an infinite stress at the boundary of the contact zone as the load is reduced and the particle removed from contact. In this case, a "neck" region is formed that prevents the unrestricted removal of the particle from contact. Scope, therefore, exists for an element of hysteresis, which could in turn affect the reliability of the data obtained relating to the nature of contact between two materials (51).

As stated, consideration must also be afforded to the nature of the chemistry at the contact point between two materials. Here we have conducted adhesion measurements using inhaled drug particles against HOPG, mica, and also particles of the same drug substance. The packing and arrangement of the budesonide molecules within the drug crystal structure were elucidated by Albertsson *et al.* (41), thus providing scope to predict key exposed chemical moieties on the crystal faces that would be principally involved during particle interaction with any substrate. With respect to the drug substance X-ray crystallographic data, it is evident that to a large extent hydrophobic groups are exposed to the immediate environment, for instance, CH_3, CH_2, and large hydrophobic sections (i.e., hydrocarbon ring structures); in addition, OH and oxygen species are exposed, although to a lesser extent. HOPG is composed of planes of carbon atoms arranged in an sp^2 hybridized format, and is known to be hydrophobic in nature (e.g., displaying a contact angle to water of 67 ± 2°; data not presented). However, if the surface properties of mica are considered, it is clear that the key surface species present in the muscovite form ($K_2Al_4(Si_6Al_2)O_{20}(OH)_4$) are oxygen, hydrogen, and potassium (52). Consequently, it may be inferred that the nature of this material is hydrophilic, where the contact angle has been determined to be less than 5° (data not shown). As a result of the aforementioned material characteristics, it should be expected that the extent of interaction between the drug particles and HOPG would be greater than with mica, this point being generally reflected in our data. This is not accounted for in the JKR model used to derive the surface energy of the drug and hence it may be expected that measurements on HOPG would lead to an overestimate of drug surface energy, as indeed is indicated in this study.

Force measurements across the predominant (002) face of the unmilled budesonide crystal enable both another method of estimation of the surface free energy for the drug material and an opportunity to directly assess local variation in this parameter. Surface energies ranging from 39 to 88 mJ m^{-2} (average value of 60 mJ m^{-2}) were derived from data recorded from different locations on the (002) face of a single crystal. Although the average of 60 mJ m^{-2} is close to that determined by IGC and a rough average of the measurements recorded from the micronized material measurements, perhaps the most intriguing implication of such data is the potential to quantitatively determine spatial variation of surface energy across single particles. It should be noted that SEM data, as shown as in Fig. 2B, reveal the large crystalline faces of the budesonide to be decorated with smaller particulates, and perhaps explain the range of observed surface energies recorded in the (002) surface that would otherwise be expected to exhibit a homogenous surface energy.

A summary of the derived surface energies for budesonide for each interacting material combination is provided in Table I.

Clearly spatial variations in the free energy term, such as observed here, may have a significant impact during both manufacture and use of the preparation. For example, it might be expected that the high-energy sites will preferentially associate with each other. This feature may considerably reduce the extent of mixing during the processing of the

Table I. A Summary of the Derived Surface Energies for Budesonide for Each Interacting Material Combination

Material combination for which adhesion is being measured		Range of derived surface energies of budesonide (mJ m^{-2})
Probe material (on AFM tip)	Substrate material	
Micronized budesonide	HOPG	35–175
Micronized budesonide	Mica	5–40
Micronized budesonide	Micronized budesonide	10–32
AFM tip (silicon nitride)	Unmilled budesonide	39–88

compound. The variation in surface energy may also significantly influence the way in which particles behave during the process of inspiration. For instance, if regions of high surface energy meet, the particles may readily aggregate and therefore result in a "particle" with a large diameter that may ultimately fail to reach the deep lung due to impaction at the back of the throat.

AFM Young's Modulus Measurements

The Young's modulus of unmilled budesonide particles was estimated from AFM nanodeformation measurements from five different particles (three areas on each) to be 10 GPa on average (with values ranging from 8 to 12 GPa). This value seems to be in agreement with previously reported values in literature, for instance, most crystalline drug and excipient substances exhibit a Young's modulus of between 5 and 10 GPa (53). For example, if we use the point beam bending method and extrapolate to zero porosity, the Young's modulus of microcrystalline cellulose shows a value of 7.5 GPa (at 22%RH) (35). Budesonide shows a value at the upper limit of this range, consistent with its observed relatively refractory nature during milling (54).

Inverse Gas Chromatography

We employed IGC to detect and quantify the surface energetic parameters of budesonide, with respect to the dispersive and specific components of the γ, for the bulk drug material of interest. The results obtained from this approach are presented in Table II. The minor differences between samples may be ascribed to factors such as variable surface crystallinity, sample purity, energetic impurities, and potential inconsistencies of surface moisture levels (32). For comparison with the AFM data, the value of the dispersive component of 68.47 ± 1.60 mJ m^{-2} is taken.

Comparison of IGC and AFM

In terms of absolute values, the ranges of surface energies observed via the various AFM strategies employed are either slightly under or encompass the value determined by IGC. It is illustrative to first consider what the outcome would be in a comparison of AFM and IGC on an "ideal sample," i.e., one that displays uniform shape, size, and energetics, and negligible mechanical deformation. Here it would be expected that the γ results obtained from AFM and IGC would be similar, within experimental error. So, it can be argued that the variability, both within each technique and when compared, is at least to a degree a function of the properties of the "real material" and hence itself represents a useful insight into the system under study. For example, the maximum values of surface energy determined by localized AFM measurements can, we propose, be related to the sites most likely to be involved in adhesion events, because the local region probed by the AFM will represent a site of relatively high surface energy compared to the surrounding surface. This type of view of the approaches employed here provides an indication as to if, and when, either AFM and/or IGC would yield the most useful information in terms of pharmaceutical analysis.

In terms of the approaches employed during this study, it is evident that key similarities and differences exist. AFM and IGC both consider only the external features of a material. The information obtained from these strategies provides scope to gain a deeper understanding of important surface parameters that can influence particulate interactions, such as topography and energetics. In addition, both AFM and IGC are quantitative techniques, thus enabling the acquisition of meaningful numerical data for use in statistical analysis to investigate a particular hypothesis or theory. Furthermore, scope exists to acquire data sets under comparable environmental conditions, hence enabling direct evaluation between the results obtained. The environmental conditions used during both the AFM and IGC studies presented here are similar; for instance, the AFM work was conducted at 25°C and 0% RH, whereas the IGC protocol was carried out at 30°C and 0% RH.

Although similarities between these strategies do exist, several differences also manifest. AFM was successfully applied here to examine particle–substrate and particle–particle interactions. In the case of AFM, only a small fraction of the total particle surface area is considered during the interaction, although as we have shown, that fraction can be selected and, to a certain extent, related to location and local topography. In contrast, IGC is typically considered to be preferentially interrogating the high-energy sites of a surface due to probe groups preferentially binding to these sites. This is probably an oversimplified view (55), but it is clear that IGC does not sample a complete surface uniformly and in quantitative terms overestimates the average surface energy of a material. In addition, clearly IGC, unlike AFM, cannot be used to study the surface energetics of single particles. This makes the direct study of the influence of fundamental forces of interaction and environmental factors on adhesion and

Table II. Surface Properties of the Drug Substance Under Investigation Determined by IGC

		$-\Delta G_{SP}$ (kJ mol^{-1})				
Sample	γ_s^d (mJ m^{-2})	Ethanol	Acetone	Ethyl acetate	Chloroform	1,4-Dioxane
1	67.45	8.71	8.01	10.39	0.56	8.40
2	70.48	8.84	8.17	10.75	0.69	8.64
3	66.94	8.61	7.83	10.42	0.52	8.41
4	69.01	8.71	7.92	10.52	0.51	8.47
Average	68.47 (1.60)	8.72 (0.09)	7.98 (0.15)	10.52 (0.16)	0.57 (0.08)	8.47 (0.11)

Each sample was acquired from the same batch. Figures in brackets represent standard deviations.

cohesion phenomena difficult. Finally, it should be noted that IGC estimates the γ in terms of dispersive and specific components and it is often difficult to unambiguously relate these parameters to allow the generation of a total γ for the material.

In general, it can be concluded that, currently, when selecting a technique to measure the interactions of drug substance with a container surface or excipients, AFM represents a good choice, particularly if the effect of environmental or storage conditions (accelerated or otherwise) are to be assessed; whereas IGC provides a better option as a quality control tool in terms of assessing whether different batches are likely to interact in a similar manner during subsequent formulation and delivery.

From a broader perspective and with respect to the various stages involved during the formulation of inhaled preparations, both AFM and IGC clearly hold promise for the in-process evaluation and assessment of particle characteristics. For instance, further to drug substance crystallization, AFM may be employed to address crystal morphology in addition to determining W_A and γ. AFM and IGC also hold promise in the investigation of the character of a preparation after the process of mixing. In relation to inhaled preparations, this process generally involves a micronized drug material being mixed with an inert carrier material, such as lactose. Here, AFM is well suited to assess the resulting topography of the drug particle–carrier material complex, altogether providing an excellent indication as to how the particles associate with each other. AFM can therefore facilitate a deeper understanding of the nature of the blend produced from the mixing process. The approach can also be readily applied to assess the carrier material to ensure suitability for use in the final presentation. IGC may be used at this stage to determine the surface energetics of the drug and carrier materials to go some way in predicting the nature and extent of interaction (e.g., low γ values for each substance would imply weak association (29)). In this way, potential carrier materials can be screened for suitability and rejected if the required criterions are not met.

CONCLUSION

The surface energy of micronized and unmilled budesonide particles was quantitatively assessed by the application of two unrelated methods, AFM and IGC. Initial work on adhesion data obtained from the AFM element of the study demonstrates a variability that can be ascribed to different contact geometries and also variation in crystal face orientation and hence chemical moieties exposed on the surface of each sample. The range of values for surface energy acquired using AFM from individual drug particle interactions with HOPG, mica, and drug particles of the same substance were found to be 35–175, 5–40, and 10–32 mJ m^{-2}, respectively. The unmilled material displayed a range of surface energy, as determined by AFM from the (002) crystal face, of 39–88 mJ m^{-2} (average value, 60 mJ m^{-2}). This observed range, which is contrary to what might be expected from the homogeneous (002) face of the crystal, probably results from smaller randomly oriented particulates distributed across the surface of the drug. The surface energy of the micronized material as determined by IGC was 68.47 ± 1.60 mJ m^{-2}.

Using force measurements acquired by the AFM has also allowed the Young's modulus of the unmilled budesonide to be determined from a single particle at a value of approximately 10 GPa. Such measurements open up possibilities of directly observing the effects of environmental factors such as humidity on a drugs mechanical properties and also the potential to spatially map at the nanoscale such properties to reveal sample heterogeneities (e.g., amorphous *vs.* crystalline states).

Potential exists to integrate the approaches taken here with other complementary techniques, such as modeling strategies, to investigate further drug particle interactions (e.g., inhaled particle–pulmonary surfactant interaction). The approach may therefore provide a deeper understanding of fundamental formulation issues governing the nature and efficacy of pulmonary drug delivery systems. We have also highlighted here that both AFM and IGC hold great potential as preformulation screening tools to assess, in a quantitative manner, the nature of drug particulate interactions and their intrinsic material properties.

ACKNOWLEDGMENTS

M.J.D. would like to thank AstraZeneca and The University of Nottingham for funding.

REFERENCES

1. D. Prime, P. J. Atkins, A. Slater, and B. Sumby. Review of dry powder inhalers. *Adv. Drug Deliv. Rev.* **26**:51–58 (1997).
2. M. E. Aulton. *Pharmaceutics—The Science of dosage Form Design*, Churchill Livingstone, New York, 1996.
3. E. R. Beach, G. W. Tormoen, J. Drelich, and R. Han. Pull-off force measurements between rough surfaces by atomic force microscopy. *J. Colloid Interface Sci.* **247**:84–99 (2002).
4. F. Podczeck, J. M. Newton, and M. B. James. Assessment of adhesion and autoadhesion forces between particles and surfaces: I. The investigation of autoadhesion phenomena of salmeterol xinafoate and lactose monohydrate particles using compacted powder surfaces. *J. Adhes. Sci. Technol.* **8**(12): 1459–1472 (1994).
5. P. M. Young, R. Price, M. J. Tobyn, M. Buttrum, and F. Dey. Investigation into the effect of humidity on drug–drug interactions using the atomic force microscope. *J. Pharm. Sci.* **92**:815–822 (2003).
6. M. Götzinger and W. Peukert. Dispersive forces of particle–surface interactions: direct AFM measurements and modelling. *Powder Technol.* **130**:102–109 (2003).
7. J. K. Eve, N. Patel, S. Y. Luk, S. J. Ebbens, and C. J. Roberts. A study of single drug particle adhesion interactions using atomic force microscopy. *Int. J. Pharm.* **238**:17–27 (2002).
8. K. K. Lam and J. M. Newton. Effect of temperature on particulate solid adhesion to a substrate surface. *Powder Technol.* **73**:117–125 (1992).
9. G. Binnig, C. F. Quate, and C. Gerber. Atomic force microscope. *Phys. Rev. Lett.* **56**:930–933 (1986).
10. M. D. Louey, P. Mulvaney, and P. J. Stewart. Characterisation of adhesional properties of lactose carriers using atomic force microscopy. *J. Pharm. Biomed. Anal.* **25**:559–567 (2001).
11. V. Bèrard, E. Lesniewska, C. Andrès, D. Pertuy, C. Laroche, and Y. Pourcelot. Dry powder inhaler: Influence of humidity on topology and adhesion studied by AFM. *Int. J. Pharm.* **232**:213–224 (2002).
12. T. Eastman and D. Zhu. Adhesion forces between surface-modified AFM tips and a mica surface. *Langmuir* **12**:2859–2862 (1996).

13. D. L. Sedin and K. L. Rowlen. Adhesion forces measured by atomic force microscopy in humid air. *Anal. Chem.* **72**:2183–2189 (2000).
14. M. Binggeli and C. M. Mate. Influence of capillary condensation of water on nanotribology studied by force microscopy. *Appl. Phys. Lett.* **65**:415–417 (1994).
15. W. A. Ducker and T. J. Senden. Measurement of forces in liquids using a force microscope. *Langmuir* **8**:1831–1836 (1992).
16. C. Vervaet and P. R. Byron. Drug–surfactant–propellant interactions in HFA formulations. *Int. J. Pharm.* **186**:13–30 (1999).
17. H. J. Butt. Measuring electrostatic, Van der Waals and hydration forces in electrolyte solutions with an atomic force microscope. *Biophys. J.* **60**:1438–1444 (1991).
18. U. Sindel and I. Zimmermann. Measurement of interaction forces between individual powder particles using an atomic force microscope. *Powder Technol.* **117**:247–254 (2001).
19. A. Relini, S. Sottini, S. Zuccotti, M. Bolognesi, A. Gliozzi, and R. Rolandi. Measurement of the surface free energy of streptavidin crystals by atomic force microscopy. *Langmuir* **19**: 2908–2912 (2003).
20. L. Zajic and G. Buckton. The use of surface energy values to predict optimum binder selection for granulations. *Int. J. Pharm.* **59**:155–164 (1990).
21. D. E. Packman. Surface energy, surface topography and adhesion. *Int. J. Adhes. Adhes.* **23**:437–448 (2003).
22. K. Kendall and C. Stainton. Adhesion and aggregation of fine particles. *Powder Technol.* **121**:223–229 (2001).
23. O. Planinšek, A. Trojak, and S. Srčič. The dispersive component of the surface free energy of powders assessed using inverse gas chromatography and contact angle measurements. *Int. J. Pharm.* **221**:211–217 (2001).
24. G. Buckton and J. M. Newton. Assessment of the wettability and surface energy of a pharmaceutical powder by liquid penetration. *J. Pharm. Pharmacol.* **37**:605–609 (1985).
25. S. Gaisford and G. Buckton. Potential applications of microcalorimetry for the study of physical processes in pharmaceuticals. *Thermochim. Acta* **380**:185–198 (2001).
26. M. A. Phipps and L. A. Mackin. Application of isothermal microcalorimetry in solid state drug development. *PSTT* **3**:9–17 (2000).
27. C. Sun and J. C. Berg. The effective surface energy of heterogeneous solids measured by inverse gas chromatography at infinite dilution. *J. Colloid Interface Sci.* **260**:443–448 (2003).
28. D. S. Keller and P. Luner. Surface energetics of calcium carbonates using inverse gas chromatography. *Colloids Surf. A: Physicochem. Eng. Asp.* **161**:401–415 (2000).
29. F. Podczeck. *Particle–Particle Adhesion in Pharmaceutical Powder Handling*, Imperial College Press, London, 1998.
30. J. C. Feeley, P. York, B. S. Sumby, and H. Dicks. Processing effects on the surface properties of α-lactose monohydrate assessed by inverse gas chromatography (IGC). *J. Mater. Sci.* **37**:217–222 (2002).
31. I. M. Grimsey, J. C. Feeley, and P. York. Analysis of the surface energy of pharmaceutical powders by inverse gas chromatography. *J. Pharm. Sci.* **92**:571–583 (2002).
32. M. D. Ticehurst, P. York, R. C. Rowe, and S. K. Dwivedi. Characterisation of the surface properties of α-lactose monohydrate with inverse gas chromatography, used to detect batch variation. *Int. J. Pharm.* **141**:93–99 (1996).
33. J. C. Feeley, P. York, B. S. Sumby, and H. Dicks. Determination of surface properties and flow characteristics of salbutamol sulphate, before and after micronisation. *Int. J. Pharm.* **172**:89–96 (1998).
34. N. M. Ahfat, G. Buckton, R. Burrows, and M. D. Ticehurst. An exploration of inter-relationships between contact angle, inverse phase gas chromatography and triboelectric charging data. *Eur. J. Pharm. Sci.* **9**:271–276 (2000).
35. B. C. Hancock, S.-D. Clas, and K. Christensen. Micro-scale measurement of the mechanical properties of compressed pharmaceutical powders: 1. The elasticity and fracture behaviour of microcrystalline cellulose. *Int. J. Pharm.* **209**:27–35 (2000).
36. C. Rotsch and M. Radmacher. Drug-induced changes of cytoskeletal structure and mechanics in fibroblasts: an atomic force microscopy study. *Biophys. J.* **78**:520–535 (2000).
37. S. C. Lieber, N. Aubry, J. Pain, G. Diaz, S. J. Kim, and S. F. Vatner. Aging increases stiffness of cardiac myocytes measured by atomic force microscopy nanoindentation. *Am. J. Physiol, Heart Circ. Physiol.* **287**:H645–H651 (2004).
38. X. M. Liang, G. Z. Mao, and K. Y. S. Ng. Mechanical properties and stability measurement of cholesterol-containing liposome on mica by atomic force microscopy. *J. Colloid Interface Sci.* **278**:53–62 (2004).
39. G. V. Lubarsky, M. R. Davidson, and R. H. Bradley. Elastic modulus, oxidation depth and adhesion force of surface modified polystyrene studied by AFM and XPS. *Surf. Sci.* **558**: 135–144 (2004).
40. Y. M. Soifer and A. Verdyan. Investigation of the local mechanical properties of potassium chloride single crystals by atomic force microscopy. *Phys. Solid State* **45**:1701–1705 (2003).
41. J. Albertsson, Á. Oskarsson, and C. Svensson. X-ray study of budesonide: molecular structures and solid solutions of the (22*S*) and (22*R*) epimers of 11β,21-dihydroxy-16α,17α-propylmethylenedioxy-1,4-pregnadiene-3,20-dione. *Acta Crystallogr., B* **34**:3027–3036 (1978).
42. J. L. Hutter and J. Bechhoefer. Calibration of atomic-force microscope tips. *Rev. Sci. Instrum.* **64**:1868–1873 (1993).
43. J. C. Hooten, C. S. German, S. Allen, M. C. Davies, C. J. Roberts, S. J. B. Tendler, and P. M. Williams. Characterization of particle-interactions by atomic force microscopy: effect of contact area. *Pharm. Res.* **20**:508–514 (2003).
44. P. M. Williams, K. M. Shakesheff, M. C. Davies, D. E. Jackson, C. J. Roberts, and S. J. B. Tendler. Blind reconstruction of scanning probe image data. *J. Vac. Sci. Technol., B* **14**:1557–1562 (1996).
45. P. M. Williams, M. C. Davies, C. J. Roberts, and S. J. B. Tendler. Noise-compliant tip-shape derivation. *Appl. Phys., A* **66**: S911–S914 (1998).
46. D. M. Schaefer, M. Carpenter, B. Gady, R. Reifenberger, L. P. Demejo, and D. S. Rimai. Surface roughness and its influence on particle adhesion using atomic force techniques. *J. Adhes. Sci. Technol.* **9**:1049–1062 (1995).
47. J. N. Israelachvili. *Intermolecular and Surface Forces*, 2nd ed. Academic Press, San Diego, 1991.
48. C. Plassard, E. Lesniewska, I. Pochard, and A. Nonat. Investigation of the surface structure and elastic properties of calcium silicate hydrates at the nanoscale. *Ultramicroscopy* **100**:331–338 (2004).
49. J. Schultz and L. Lavielle. Interfacial properties of carbon fibre–epoxy matrix composites. In D. R. Lloyd, T. C. Ward, and H. P. Schreiber (eds.), *Inverse Gas Chromatography Characterisation of Polymers and other Materials; ACS Symp. Ser. 391*, American Chemical Society, Washington, DC, 1989, pp. 185–202.
50. K. L. Johnson, K. Kendall, and A. D. Roberts. Surface energy and the contact of elastic solids. *Proc. R. Soc. Lond., A* **324**:301–313 (1971).
51. E. R. Beach, G. W. Tormoen, and J. Drelich. Pull-off forces measured between hexadecanethiol self-assembled monolayers in air using an atomic force microscope: analysis of surface free energy. *J. Adhes. Sci. Technol.* **16**:845–868 (2002).
52. S. G. Barlow and D. A. Manning. Influence of time and temperature in reactions and transformations of muscovite mica. *Br. Ceram. Trans.* **98**:122–126 (1999).
53. R. J. Roberts, R. C. Rowe, and P. York. The relationship between Young's modulus of elasticity of organic solids and their molecular structure. *Powder Technol.* **65**:139–146 (1991).
54. AstraZeneca, personal communication.
55. H. E. Newell and G. Buckton. Inverse gas chromatography: investigating whether the technique preferentially probes high energy sites for mixtures of crystalline and amorphous lactose. *Pharm. Res.* **21**:1440–1444 (2004).